

Noncollinear magnetic ordering in compressed FePd₃ ordered alloy: A first principles studyY. O. Kvashnin,¹ S. Khmelevskiy,² J. Kudrnovský,³ A. N. Yaresko,⁴ L. Genovese,^{1,5} and P. Bruno¹¹European Synchrotron Radiation Facility, 6 Rue Jules Horowitz, BP 220, 38043 Grenoble Cedex, France²Vienna University of Technology, CMS, Institute for Applied Physics, AT-1020 Vienna, Austria³Institute of Physics, Academy of Sciences of the Czech Republic, Na Slovance 2, CZ-182 21 Prague, Czech Republic⁴Max-Planck-Institut für Festkörperforschung, Heisenbergstrasse 1, D-70569 Stuttgart, Germany⁵Laboratoire de Simulation Atomistique, SP2M, UMR-E CEA/UJF-Grenoble 1, INAC, Grenoble, F-38054, France

(Received 19 October 2012; published 29 November 2012)

By means of *ab initio* calculations based on the density functional theory we investigated the magnetic phase diagram of ordered FePd₃ alloy as a function of external pressure. Considering several magnetic configurations we concluded that the system under pressure has a tendency toward noncollinear spin alignment. Analysis of the Heisenberg exchange parameters J_{ij} revealed strong dependence of iron-iron magnetic couplings on polarization of Pd atoms. To take into account that effect we built an extended Heisenberg model with higher order (biquadratic) terms. Minimizing the energy of this Hamiltonian, fully parametrized using the results of *ab initio* calculations, we found a candidate for a ground state of compressed FePd₃, which can be seen as two interpenetrating “triple-Q” phases.

DOI: [10.1103/PhysRevB.86.174429](https://doi.org/10.1103/PhysRevB.86.174429)

PACS number(s): 75.25.-j, 75.30.Et, 75.50.Bb, 71.20.Be

I. INTRODUCTION

Magnetism of Fe alloys is a long standing problem in solid state physics having fundamental importance for modern technology.¹ One of the big challenges is understanding magnetism of iron on a face-centered cubic (fcc) lattice, which is a key issue toward comprehension of a variety of phenomena, such as spin glass behavior, the Invar anomaly, and a quantitative description of structural transition in steels.

In pure γ -Fe first principles calculations predict the stabilization of the spin spiral state.² More generally it has been shown that, for a number of disordered fcc Fe-based binary alloys, such as Fe-Ni and Fe-Pt, the sign of the effective magnetic interaction (ferro- or antiferromagnetic) is dependent on the volume, being ferromagnetic at larger volumes and antiferromagnetic at lower ones.^{3–5} The antiferromagnetic interactions on frustrated and chemically disordered lattices lead to the appearance of noncollinear ground states (GSs) at certain region of volumes, as predicted in work by van Schilfhaarde *et al.*⁶ Indeed it was shown theoretically that this volume region can be reached under applied pressure.^{7,8}

Thanks to the use of diamond anvil cells at synchrotron facilities it has become possible to measure x-ray spectra and investigate properties of matter under extremely high pressure. In today's experiments the values of applied pressure exceed the 100 GPa range, giving an opportunity to study ordinary compounds in unconventional conditions. It is of particular interest to investigate Fe-based transition metals alloys under pressure due to the above mentioned volume-dependent magnetic peculiarities of their behavior. A couple of experiments at ultrahigh pressures have been performed on disordered Invar Fe-Ni alloys^{9–12} as well as on Fe₃C cementite.¹³ In particular, the results of these experiments suggest the stabilization of a spin-glass state under pressure in Fe-Ni and Fe-Pt alloys^{10,11} and an abrupt change of the magnetic state under some pressure (magnetovolume instability), which is in general consistent with the prediction of a sharp variation of exchange couplings with pressure in these systems.^{3,4,14}

FePd₃ alloy has recently attracted strong interest due to its Invar behavior. It was observed experimentally that under an applied pressure of 7 GPa the system shows an anomalously small thermal expansion.¹⁵ Hence the considered compound demonstrates a pressure-induced Invar effect, reminiscent that of Fe₅₀Ni₅₀ disordered alloy.⁹ Moreover, as will be shown below, noncollinear spin states are stabilized in FePd₃ at low volumes, similarly to the Fe₅₀Ni₅₀ case.

Winterrose *et al.*¹⁵ investigated FePd₃ under pressure from both experimental and theoretical viewpoints. Results of x-ray diffraction measurements implied that under the pressure of 12 GPa the system undergoes a significant volume collapse while preserving its Cu₃Au (L1₂) structure. Moreover, under the same applied pressure they observed a disappearance of quantum beats in a nuclear forward scattering (NFS) experiment, which indicates the loss of long-range magnetic order in the system. In order to interpret the results, authors performed a set of supercell calculations, based on density functional theory (DFT), for a few possible magnetic configurations. By comparing elastic properties of different states with experimental data, they came to the conclusion that there is a high-spin (HS) to low-spin (LS) transition taking place under pressure. This hypothesis is supported by the fact that the obtained magnetic moments in the LS state are of the order of $10^{-2}\mu_B$, and this can explain the loss of signal in the NFS experiment. On the other hand, the LS phase never had lower total energy than the ferromagnetic (FM) state in a considered volume range. However, the possibility of paramagnetic case, i.e., the Curie point under pressure being below room temperature, cannot be simply excluded.

FePd₃ is a complex magnetic system, because it is composed of rather localized (Fe) and itinerant (Pd) magnetic moments. One of the first attempts to account for coexisting magnetism of different characters was carried out by Mohn and Schwarz.¹⁶ They proposed a model where local spins produced an effective Weiss field acting on an itinerant

magnetic sublattice. The parametrization of the model was based on the results of *ab initio* calculations. The developed model was applied for Pd-rich $\text{Fe}_x\text{Pd}_{1-x}$ ($x < 0.1$) alloys and estimated Curie temperatures (T_c) were found to be in good agreement with experiment.

The problem of induced moments and their influence on magnetic properties of some Fe-containing alloys was studied in a series of publications by Mryasov *et al.*^{17,18} For example, it was pointed out that polarized Pt atoms are responsible for anomalous temperature behavior of magnetocrystalline anisotropy in FePt. Also, the induced magnetization on Rh atoms was shown to play crucial role in the phase stability of FeRh.

An extensive first principles study of iron-palladium compounds was made by Burzo *et al.*¹⁹ Their authors performed calculations using scalar relativistic tight-binding linear muffin-tin orbital (TB-LMTO) method.²⁰ The reported values of equilibrium lattice constant and magnetic moments were in good agreement with available experimental data. A rough estimation of T_c for different Pd concentrations using a mean field approximation (MFA) was not successful, yielding a too low value (while MFA should normally overestimate the result).

A more accurate approach for calculating T_c in Fe-Pd solutions and compounds was proposed in Ref. 21. Pd magnetization was considered to be proportional to the vector sum of neighboring magnetic moments. The suggested computational scheme was based on the extended Heisenberg Hamiltonian with exchange parameters extracted from self-consistent *ab initio* calculation.

Recently another group reported a theoretical study of the magnetism of FePd_3 under applied pressure.²² The authors explored various chemically and magnetically disordered states and came to the conclusion that those states cannot be the candidates for a GS of the system. On the other hand they observed a strong competition between commensurate (FM, AFM) and incommensurate [spin spiral (SS)] magnetic configurations. The authors suggest that this is an indication that the system might undergo a transition to some noncollinear state upon the application of pressure.

Mainly motivated by the results of Winterrose *et al.*,¹⁵ in the present work we will show a possible GS of ordered FePd_3 under pressure and discuss the origins of the magnetic transition.

II. METHODS

In order to have a realistic description of electronic structure of the studied system we carried out a set of self-consistent DFT calculations using PY-LMTO code.²³ Correlation effects were treated within a local spin density approximation (LSDA) with the parametrization of Vosko, Wilk, and Nusair.²⁴

The crystalline structure of the compound under consideration is depicted in Fig. 1. In the present study we were interested in finding a magnetic GS of compressed FePd_3 . It is certainly impossible to explore all magnetic configurations, as there are an infinite number of them. Thus we have investigated the most plausible candidates for the GS by comparing their total energies and examining their stability with respect to

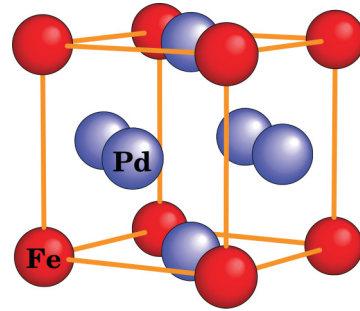


FIG. 1. (Color online) Schematic representation of ordered FePd_3 . The alloy has a fcc-based $L1_2$ structure, where Fe atoms are located at the corners of the cube and Pd atoms are at the centers of the faces.

infinitesimal deviations of magnetic moment orientations, keeping in mind that this is a probe of the local stability and not the global one.

First we considered possible SS states. These simulations were carried out on the basis of the generalized Bloch theorem,²⁵ allowing us to avoid laborious supercell calculations. Note that these calculations are scalar relativistic, and therefore there is no coupling between spin degrees of freedom and the crystal lattice. Due to the presence of a global spin rotational invariance, the direction of the quantization axis can be chosen arbitrarily. We will align it along the z axis. Hence SS states are defined by four parameters: the propagation vector [$\mathbf{Q} = (q_x, q_y, q_z)$] and the angle Θ formed by magnetization and the z axis. Once these parameters are chosen, the magnetization of the iron atom in neighboring cell is rotated by an angle $\phi_i = \mathbf{Q} \cdot \mathbf{R}$, where \mathbf{R} denotes a translational vector. Initial phases of Pd moments located at positions \mathbf{t}_i were set to $\phi_i^0 = \mathbf{q} \cdot \mathbf{t}_i$, but were allowed to choose preferred orientation during a self-consistent loop. SS calculations are shown in Sec. IV.

Consideration of more complex magnetic phases required construction of appropriate supercells. In order to accommodate some spin structures, we had to use cells containing up to eight formula units. The directions of iron magnetic moments were prescribed and frozen during these calculations. This was done so because the differences in energies associated with spin deviations were rather small ($\sim \text{meV}$), so the total energy profile is very shallow in this direction and in addition possesses plenty of local minima. Due to the induced character of Pd magnetic moments, their directions and magnitudes were obtained fully self-consistently. The corresponding calculations are described in Secs. V and VI.

The high-temperature paramagnetic (PM) state was modeled by a disordered local moment (DLM)²⁶ configuration. The effect of magnetic disorder was taken into account by the coherent potential approximation (CPA), as implemented in TB-LMTO-CPA.²⁷ The DLM approach is used to describe properties of the system consisting of randomly distributed magnetic impurities embedded in a nonmagnetic medium. Thus induced magnetization on nonmagnetic ions, which is a result of an overlap with spin-polarized bands originating from magnetic atoms, collapses to zero in this phase. Therefore, such an approach can be a useful tool for understanding the nature of magnetic moments.

In order to get a deeper insight into magnetic properties, we mapped our system on a classical Heisenberg model of the following form:

$$\hat{H}_{\text{exch}} = - \sum_{i \neq j} J_{ij} \mathbf{e}_i \cdot \mathbf{e}_j, \quad (1)$$

where J_{ij} denotes the exchange integral between magnetic atoms at sites i and j , and \mathbf{e}_i and \mathbf{e}_j are unit vectors in the directions of the local magnetization on sites i and j , respectively. Exchange parameters were computed using the approach of Lichtenstein *et al.* based on magnetic force theorem.²⁸

$$J_{ij} = \frac{1}{4\pi} \Im \int_{-\infty}^{E_f} \text{Tr}(\Delta_i G_{ij}^{\uparrow} \Delta_j G_{ji}^{\downarrow}) d\varepsilon, \quad (2)$$

where Δ_i is an exchange potential on the i th site and G_{ij}^{σ} is an intersite Green's function, which describes propagation of an electron with spin $\sigma = \{\uparrow, \downarrow\}$ from site i to j . Within this method, exchange integrals between two sites are calculated as a response to infinitesimally small deviations of corresponding magnetic moments away from the reference state. So the assumed magnetic order matters and, as will be shown later, the effective J_{ij} parameters can be different for various states. The consequences of this will be discussed in more detail in Sec. III. In order to probe the stability of a certain magnetic state, extracted J 's were used to find low-energy magnetic excitation (i.e., frozen magnon) spectra, which are the eigenmodes of a considered Hamiltonian. A more detailed description of the computational aspects can be found elsewhere.²⁹

It has to be mentioned that the equilibrium volume value and corresponding pressures predicted by LSDA are different from the experimental ones. In most of the cases LSDA leads to underestimation of the bond length by a few percent.³⁰ To avoid any ambiguity, we will work with an experimental lattice parameter for FePd₃, which is 3.849 Å at ambient conditions,^{15,31} and its corresponding volume V_0 is used throughout the paper.

III. HEISENBERG EXCHANGE INTERACTIONS

Self-consistent calculations for the DLM state were carried out in TB-LMTO-CPA. It is found that Fe atoms keep the values of their moments in DLM (PM) state almost unchanged compared to the magnetically ordered states, thus suggesting a high degree of localization of the iron magnetic moment. The difference in absolute values of M_{Fe} in DLM and FM states at equilibrium volume was approximately 2%. The same correspondence holds under applied pressure and thus there is no tendency toward a drop of the magnetic moment as suggested by the HS-LS scenario.¹⁵ Similar results were already reported in a previous study.²²

Using obtained TB parameters, we have calculated pair exchange integrals starting from the DLM state. In this case Fe moments do not have any prescribed orientation and extracted J parameters should reflect the properties of the system in the high-temperature phase above T_c . This approach was successfully applied in previous studies.^{32,33}

It should be mentioned, however, that application of the magnetic force theorem to systems with induced local

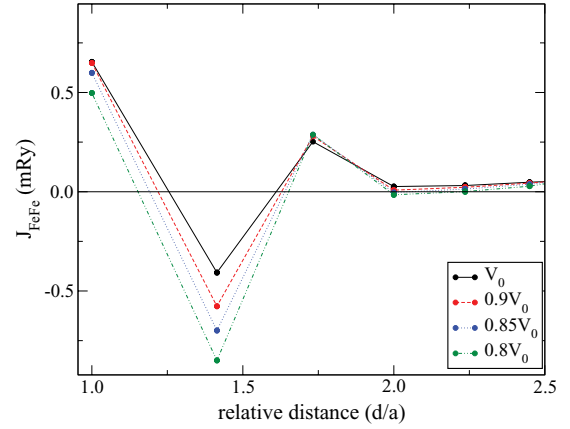


FIG. 2. (Color online) The Fe-Fe exchange interactions in FePd₃ as functions of the relative interatomic distance d/a , where a is the lattice parameter. Results were obtained from the DLM reference state calculated for different cell compressions.

moments has limited validity, as was shown by Sandratskii *et al.*³⁴ In the DLM state small induced Pd moments are reduced to zero due to random orientations of Fe spins. We therefore investigate a net effect of iron moments on possible magnetic ground states which may exist at low temperatures.

In Fig. 2 we show calculated effective J_{FeFe} parameters as a function of interatomic distance for a few fractions of equilibrium volume. The results suggest that the first and second nearest-neighbor (NN) interactions are dominant. While the first NN interactions (6 neighbors) are FM, the second NN (12 neighbors) couplings are AFM. Third NN exchange parameters, which are FM, are also important. Such oscillatory behavior is due to the Ruderman-Kittel-Kasuya-Yosida (RKKY)³⁵ nature of exchange interactions in metals and is similar to that reported for bcc Fe.²⁹

We report a strong increase of second NN AFM interactions with pressure while all other couplings depend on volume much more weakly. Moreover, the corresponding neighborhood forms the fcc lattice, which is frustrated for this sign of interaction. Here we found that the frustration, being a natural source of noncollinearity in spin systems, effectively increases its contribution at lower volumes. We will refer to this fact in the next section.

Next we examined the stability of several magnetic states in compressed FePd₃. In Fig. 3 we show the calculated iron-iron J_{FeFe} exchange parameters extracted from DLM and AFM [110] states. Using the obtained parameters, we computed frozen magnon spectra for each of these states. However, all phases demonstrated local magnetic instabilities, indicating that any small perturbation would destroy the state. In other words all these magnetic configurations are not even local minima on a phase diagram of the system under consideration. Nonetheless, we obtained important information: the Fe spins have a tendency toward noncollinearity. Motivated by this fact, we examined the energies of spin spiral and other noncollinear states.

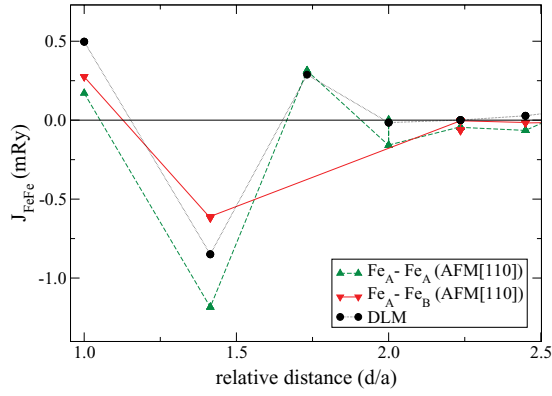


FIG. 3. (Color online) Iron-iron exchange parameters obtained from DLM and AFM [110] states for $0.8V_0$. Two iron sublattices which appear in the AFM [110] state are denoted as Fe_A and Fe_B .

IV. SPIN SPIRAL CALCULATION

First we explored the manifold of the states characterized by $\Theta = 90^\circ$. The energies of these states as a function of wave vector are shown in Fig. 4. The results imply that for ambient pressure the Γ point has the lowest energy among all considered configurations. This is a manifestation of the stability of the FM state.

Nevertheless, there are two local minima at X and M high symmetry points. These points correspond to antiferromagnetic (AFM) states with ordering vectors $[100]$ and $[110]$, respectively. One additional minimum is lying along the Γ - R direction and corresponds to wave vector $\mathbf{q} = (\frac{\pi}{2a}, \frac{\pi}{2a}, \frac{\pi}{2a})$. Such peculiarities of the total energy were already emphasized by another research group.²² The overall shape of the energy profile is in fair agreement with those calculations, even though different computational schemes were used.

It is seen that with increasing pressure the stability of the FM state is reduced, and at a volume of about $0.88V_0$ we observe the magnetic transition at the point M corresponding to the AFM [110] phase, as was previously reported by Winterrose *et al.*¹⁵ Further compression leads to further destabilization of the ferromagnetic configuration.

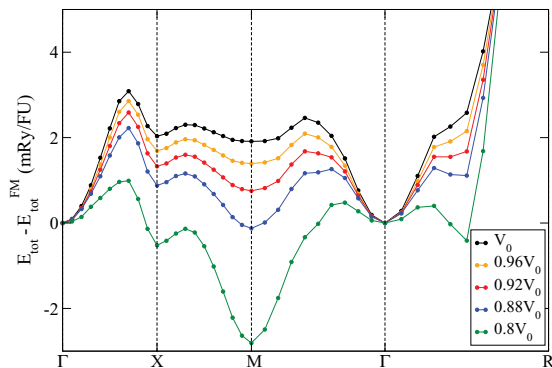


FIG. 4. (Color online) Total energies of spin spiral states relative to the energy of the FM state at a given volume in $FePd_3$. R - X and R - M directions are not shown, as wave-vector dependence of the total energy was found to be monotonic along these paths. The energies are given per chemical formula unit (FU).

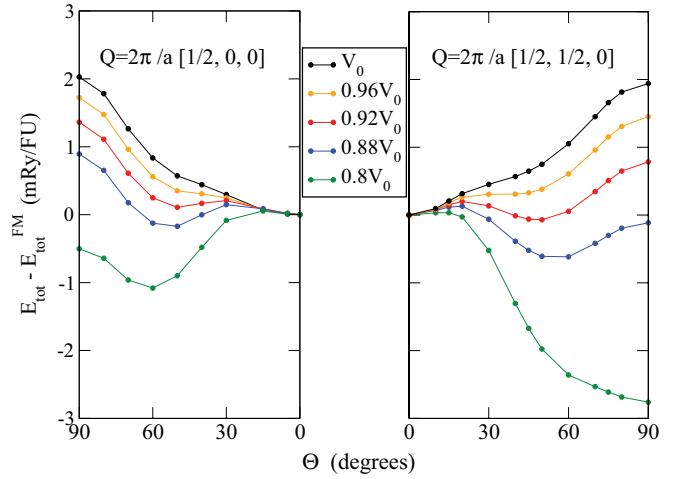


FIG. 5. (Color online) Energies of helical spin configurations as a function of the angle between magnetization and the z axis in $FePd_3$. Values are relative to the energy of the FM state at a given volume.

It should be noted that iron has a quite rigid magnetic moment in entire considered volume range: For a majority of configurations, as volume is decreased by 20%, its magnetization M_{Fe} lowers by not more than 11%.

Another remarkable fact is that, for a fixed volume, the magnitude of the iron magnetic moment has very similar values among different SS states. The highest difference was observed between FM and AFM [110] states and was estimated to be $\approx 0.1\mu_B$ per atom. Meanwhile the value of M_{Pd} strongly depends on its environment, as was already pointed out by another group.²¹ For example, at volume V_0 in the FM state all Pd ions possess magnetic moment of $\approx 0.35\mu_B$ per atom. In the layered AFM [100] state Pd atoms that belong to the same layer as Fe atoms have a magnetization of $0.14\mu_B$ per atom, pointing parallel to the iron moment. The remaining palladium atoms are nonmagnetic. In the AFM [110] state all Pd moments collapse to zero, because each of them is surrounded by an equal number of Fe moments pointing “up” (Fe_A) and “down” (Fe_B).

Our next step was an investigation of various helical structures. In this set of calculations we have chosen two \mathbf{Q} vectors, corresponding to the lowest states observed so far, namely AFM [100] and AFM [110]. Freezing these three parameters of the SS states, we tried to vary the value of the Θ angle. Energies of such magnetic structures are shown in Fig. 5. The results again suggest a reduction of the FM stability with increasing pressure, but for both studied directions (\mathbf{Q}) we observed a wide range of volumes where helical states are in favor. As one compresses the cell up to $0.92V_0$ the FM phase becomes almost degenerate with two more states, which in the coordinate system (\mathbf{Q}, Θ) correspond to the points $(X, 50^\circ)$ and $(M, 50^\circ)$. Further volume decrease leads to the destabilization of the FM solution and the states belonging to the family (M, α) possess the lowest energy in the entire volume range.

At $0.8V_0$ the AFM [110] phase possesses the lowest energy among spin-polarized states. However, we have already pointed out that the calculated frozen magnon dispersion indicated a local instability of this state, i.e., the appearance of imaginary eigenvalues in the corresponding spectrum. Therefore we deduced that this is not a GS and this fact forced

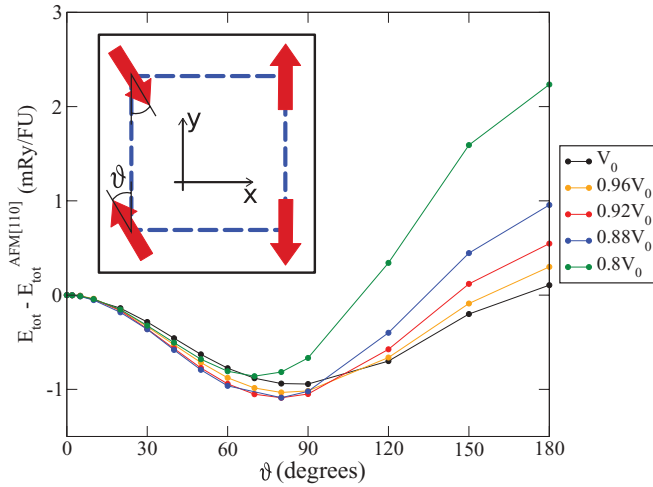


FIG. 6. (Color online) Results of the total energy DFT calculations of canted states in ordered FePd₃. The inset shows the magnetic structure under consideration. Red arrows indicate iron magnetic moments. Pd magnetization is not shown.

us to investigate more complex states. Moreover, so far we have considered only coplanar spin structures.

V. CANTED SPIN STATES

In order to explore more complex magnetic states, we constructed a $2 \times 2 \times 1$ supercell of FePd₃ with four nonequivalent iron sublattices. Here we introduce an angle θ for iron spins, defined as shown in the inset of Fig. 6. Thus $\theta = 0$ corresponds to the AFM [110] phase and $\theta = 180^\circ$ to AFM [100]. By tuning θ one can go continuously from one state to another. At each volume the calculations were carried out for the angle θ fixed to a given value. A fully unconstrained determination of θ would be an extremely difficult task, due to the reasons mentioned in Sec. II.

According to the obtained results, the corresponding function $E_{\text{tot}}(\theta)$, in addition to the points $\theta = \{0, 180^\circ\}$, has one more minimum at a certain angle (θ_0). Such angular dependence cannot be accounted for within a classical Heisenberg picture, which should give a “cos(θ)” curvature. Note that the present shape of the total energy profile was found even without inclusion of spin-orbit coupling (SOC). Thus relativistic effects, such as magnetic anisotropy, are not responsible for such behavior. The situation is reminiscent of the study of iron pnictides,³⁶ where similar constrained calculations were performed. For that case it was proposed that the proper $E_{\text{tot}}(\theta)$ dependence can be obtained by introducing higher-order exchange terms to the spin model.

Following this idea, we have built an extended Heisenberg-like model, which aims to catch the essential physical properties of FePd₃ and guide us toward finding a true ground state.

VI. EXTENDED HEISENBERG MODEL AND TRIPLE-Q STRUCTURE

The influence of Pd moments on stability of the FM state is crucial, as was demonstrated by Polesya *et al.*,²¹ and therefore it is essential to take them into account.

Palladium is a rather peculiar element: it is known that bulk Pd is characterized by a high density of states at the Fermi level, so the Stoner criterion is nearly satisfied. Therefore Pd is easily polarized by contact with neighboring magnetic moments. Certainly it participates in magnetic interactions, and as a result effective couplings between two iron sites in the FM phase, where Pd gets polarized, and in AFM one, where it is nonmagnetic, are considerably different (Fig. 3).

The underlying physics can be understood by looking at the expression of the J parameters in Eq. (2). Since the magnitude of Fe magnetic moment is almost configuration independent, one gets that $|\Delta_{\text{Fe}}|$ is approximately the same in all states. Therefore what gives rise to the observed difference in exchange couplings is the intersite Green’s function. In the FM state an electron, going from one iron site to another, propagates through a strongly polarized medium, while in the AFM state this polarization is missing. Since Pd magnetization is large ($\sim 0.3\mu_B$ per atom), being a first-order term in Δ_{Fe} , its disappearance has a significant impact on G_{ij} and eventually on exchange integrals. As a result a classical Heisenberg model, with pairwise interactions and bilinear exchange only, cannot properly map the dependence of the total energy on the magnetic configurations and must be extended to include higher-order exchange terms.

Such behavior was already reported for an FeRh compound.¹⁸ It is worth emphasizing that this situation is not generic and can be ascribed to be the feature of these $4d$ elements. In order to stress this point, we performed additional calculations for a hypothetical system, where palladium was substituted by copper atoms within same geometry of the unit cell. Opposite to the previous case, Cu is nonmagnetic in both AFM [110] and FM states. In this case we found that J_2 parameters extracted from both configurations almost coincide with each other. Thus we do not observe any pronounced deviations from the Heisenberg magnet behavior.

Hence, in order to take into account such peculiarities of the magnetic interactions, we propose an effective model for iron degrees of freedom, which in addition to Eq. (1) contains higher-order exchange terms, originating from the polarization of palladium atoms:

$$\hat{H} = \hat{H}_{\text{exch}} - \sum_{i \neq j} J'_{ij} (\mathbf{e}_i \cdot \mathbf{e}_j)^2, \quad (3)$$

where J' is a biquadratic exchange parameter.

Thus we are able to build a Heisenberg-like model and fully parametrize it using the results of DFT calculations. For simplicity we considered interactions with the first three coordination spheres (J_1, J_2, J_3) only, as the remainder are much smaller. As was already pointed out, the Pd-originated renormalization of J parameters is the most pronounced for next NNs (J_2), and therefore we introduce a biquadratic term only for this coupling.³⁷ The values which were extracted from Fig. 3 and used for the model are the following: $\{J_1, J_2, J'_2, J_3\} \rightarrow \{0.236, -0.902, -0.282, 0.29\}$ (in mRy). It is seen that J'_2 is of the same order as bilinear exchange. Such a situation is atypical, but not unique: for example, a sizable value of the biquadratic term is necessary to explain properties of another class of Fe-based materials.³⁸ Moreover, the present set of parameters describes well the

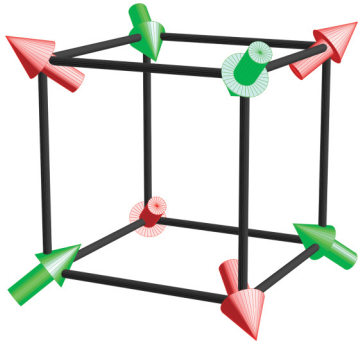


FIG. 7. (Color online) Obtained high-pressure magnetic phase of FePd_3 . Arrows represent iron magnetic moments. Four spins of the same color, forming the triple- Q state, point toward the center of the cube; four others point opposite to it. Note, that the state is degenerate with respect to simultaneous rotations of all spins through the same angles.

curvature of the $E_{\text{tot}}(\theta)$ profile, shown in Fig. 6. The very existence of the minimum θ_0 as well as its position are in fair agreement with those calculations. This can be viewed as an indication of plausibility of the chosen parameters for our model.

Minimizing the energy of the Hamiltonian [Eq. (3)] on a $2 \times 2 \times 2$ supercell, we obtained a new ground state of the system, which is depicted in Fig. 7. The magnetic structure of this state can be seen as two interpenetrating fcc subsystems, whose spins form so-called triple- Q ($3Q$) states.³⁹ The angle between each pair of spins is $109^\circ 28'$, hence the vectors point toward the vertices of an ideal tetrahedron. Each spin out of eight has an identical pair, so its vertices are twice degenerate. Analysis of the spin arrangement revealed that J_3 coupling (FM), which connects two fcc sublattices, is fully satisfied within such a geometry. The rest of the interactions compete with each other due to the presence of frustration in the system. Note that negative sign of J_2' means that the interaction favors perpendicular spin orientation. This term is the driving force lifting the degeneracy associated with the frustration, and results in stabilization of a certain angle between spins.

It was shown before for fcc-based alloys that stability of triple- Q state with respect to single- Q ones can be related to nonlinear spin interactions in the system⁴⁰ and/or the presence of paramagnetic impurities.⁴¹ In fact, both of these ingredients are presented in FePd_3 , and hence our findings are consistent with the established physical picture. However, to the best of our knowledge the presented spin structure was not observed in alloys with such a low concentration of magnetic ions.

In order to check the stability of the obtained configuration, we have computed the corresponding dispersion of low-energy magnetic excitations (Fig. 8). First of all we confirm that all excitations have a positive energy, meaning that the state is stable. It is worth emphasizing once again that all states which were studied before showed instabilities in their spectra. Second, one can see few almost degenerate Goldstone modes obeying a linear dispersion law at small values of the wave vector \mathbf{q} . We will refer to this fact in the next section.

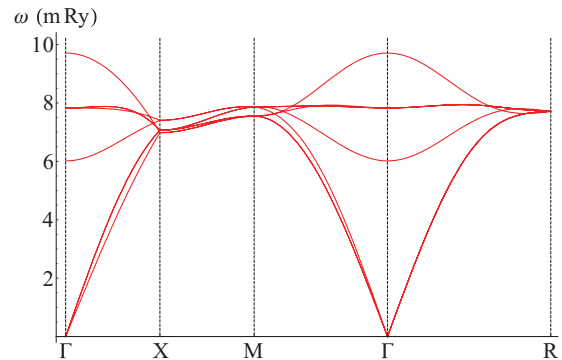


FIG. 8. (Color online) Frozen magnon energies of the proposed high-pressure magnetic phase of FePd_3 .

Finally, we carried out a total-energy DFT calculation of the $3Q$ state for different fractions of equilibrium volume. It was confirmed that this noncollinear state becomes lower in energy than the FM one at a relative compression rate of 0.96, which is in excellent agreement with the experiment.¹⁵ The triple- Q state possesses the lowest energy among all studied states in the low-volume region.⁴²

Hence we see that the model with the present choice of J parameters describes well the properties of the system next to the GS. It has to be mentioned, however, that this set is unable to reproduce the relative energies of spin spirals depicted in Fig. 4. One possible explanation is that incommensurate spin states possess a significant Pd magnetization which has to be taken into account explicitly for a proper energy estimation.

VII. OBSERVATION OF THE TRIPLE- Q STATE

$3Q$ states are rather difficult to observe experimentally, because their behavior is similar to collinear antiferromagnets.⁴³ The measurement which helped to distinguish these two phases was proposed by Kawarazaki *et al.*⁴⁴ The method, however, requires certain elements which are the sources of the γ rays. Thus for the case of FePd_3 a more useful way would be to use the Mössbauer effect in Fe, but this technique cannot provide an unequivocal answer if the state is more complex than single- Q type.⁴⁵

As was already pointed out, first of all we suspect that there should be an abrupt change in the shape of the spin-wave dispersion from parabolic to linear in FePd_3 under applied pressure. This would be the first indication of existence of the triple- Q state, which is necessary, but not sufficient.

Another external parameter which has to be controlled during an experiment is the temperature. In Ref. 15 a complete vanishing of Fe average magnetization was found in the NFS experiment upon compression. One of explanations is that the value of T_c is strongly affected by applied pressure and at a given volume it is pushed below room temperature. However, a reliable *ab initio* evaluation of T_c of FM FePd_3 would be already a difficult task and seems not to be solved in the previous studies.^{19,21} Recent results on estimation of T_c in MFA confirm its decrease upon the application of pressure,²² but it seems to reach room temperature at lower volumes than

observed experimentally. It should not be excluded that $3Q$ configuration might have a different ordering temperature as compared with the FM one. This is one explanation of the loss of the NFS signal.

Another issue with such type of systems is disorder. Ordered FePd₃ samples are obtained by annealing and subsequent fast cooling (quenching). Hence some amount of residual disorder can always appear in a real system. It was reported that the value of transition pressure differs from one sample to another.⁴⁶ This fact may suggest that a small antisite disorder is present and can affect a phase diagram of the compound under consideration. In principle, this can give rise to more complicated spin structures.

VIII. CONCLUSIONS

We have studied theoretically the ground-state magnetic properties of FePd₃ ordered alloy under external pressure using first principles methods. It was deduced that the compound

undergoes a magnetic transition from the FM to the triple- Q state at 0.96 fraction of equilibrium volume. Fe atoms possess a significant magnetic moment in the high-pressure phase, unlike the HS-LS scenario suggested earlier. The disappearance of the quantum beats in the NFS experiment¹⁵ may indicate a drop of T_c across the transition. Essential ingredients which stabilize the $3Q$ states can be determined: (i) an existence of strong magnetically frustrated couplings in the system, which is J_2 in the present case; and (ii) admixture of higher-order interactions, favoring perpendicular spin alignment.

ACKNOWLEDGMENT

J.K. acknowledges financial support from the Czech Science Foundations (P204/11/1228) and S.K. acknowledges support from the Austrian Science Fund (FWF) (SFB ViCoM F4109-N13). Y.O.K. thanks the Institute of Physics (Prague) for hospitality during his stay.

-
- ¹W. Pepperhoff and M. Acet, *Constitution and Magnetism of Iron and its Alloys* (Springer-Verlag, Berlin, 2001).
- ²L. M. Sandratskii, *Adv. Phys.* **47**, 91 (1998).
- ³W. Olovsson and I. A. Abrikosov, *J. Appl. Phys.* **97**, 10A317 (2005).
- ⁴A. V. Ruban, M. I. Katsnelson, W. Olovsson, S. I. Simak, and I. A. Abrikosov, *Phys. Rev. B* **71**, 054402 (2005).
- ⁵S. Khmelevskiy and P. Mohn, *Phys. Rev. B* **68**, 214412 (2003).
- ⁶M. van Schilfhaarde, I. Abrikosov, and B. Johansson, *Nature (London)* **400**, 46 (1999).
- ⁷I. A. Abrikosov, A. E. Kissavos, F. Liot, B. Alling, S. I. Simak, O. Peil, and A. V. Ruban, *Phys. Rev. B* **76**, 014434 (2007).
- ⁸A. V. Ruban, S. Khmelevskiy, P. Mohn, and B. Johansson, *Phys. Rev. B* **76**, 014420 (2007).
- ⁹L. Dubrovinsky, N. Dubrovinskaja, I. A. Abrikosov, M. Vennström, F. Westman, S. Carlson, M. van Schilfhaarde, and B. Johansson, *Phys. Rev. Lett.* **86**, 4851 (2001).
- ¹⁰M. Matsushita, S. Endo, K. Miura, and F. Ono, *J. Magn. Magn. Mater.* **265**, 352 (2003).
- ¹¹M. Matsushita, S. Endo, K. Miura, and F. Ono, *J. Magn. Magn. Mater.* **260**, 371 (2003).
- ¹²F. Decamps and L. Nataf, *Phys. Rev. Lett.* **92**, 157204 (2004).
- ¹³E. Duman, M. Acet, E. F. Wassermann, J. P. Itié, F. Baudet, O. Mathon, and S. Pascarelli, *Phys. Rev. Lett.* **94**, 075502 (2005).
- ¹⁴S. Khmelevskiy and P. Mohn, *Phys. Rev. B* **82**, 134402 (2010).
- ¹⁵M. L. Winterrose, M. S. Lucas, A. F. Yue, I. Halevy, L. Mauger, J. A. Muñoz, J. Hu, M. Lerche, and B. Fultz, *Phys. Rev. Lett.* **102**, 237202 (2009).
- ¹⁶P. Mohn and K. Schwarz, *J. Phys: Condens. Matter* **5**, 5099 (1993).
- ¹⁷O. N. Mryasov, U. Nowak, K. Y. Guslienko, and R. W. Chantrell, *Europhys. Lett.* **69**, 805 (2005).
- ¹⁸O. N. Mryasov, *Phase Transitions* **78**, 197 (2005).
- ¹⁹E. Burzo and P. Vlaić, *J. Optoelectron. Adv. Mater* **12**, 1869 (2010).
- ²⁰O. K. Andersen and O. Jepsen, *Phys. Rev. Lett.* **53**, 2571 (1984).
- ²¹S. Polesya, S. Mankovsky, O. Sipr, W. Meindl, C. Strunk, and H. Ebert, *Phys. Rev. B* **82**, 214409 (2010).
- ²²B. Dutta, S. Bhandary, S. Ghosh, and B. Sanyal, *Phys. Rev. B* **86**, 024419 (2012).
- ²³V. Antonov, B. Harmon, and A. Yaresko, *Electronic Structure and Magneto-Optical Properties of Solids* (Kluwer Academic, Dordrecht, 2004).
- ²⁴S. H. Vosko, L. Wilk, and M. Nusair, *Can. J. Phys.* **58**, 1200 (1980).
- ²⁵L. M. Sandratskii, *J. Phys. Condens. Matter* **3**, 8565 (1991).
- ²⁶B. Gyorffy, A. Pindor, J. Staunton, G. Stocks, and H. Winter, *J. Phys. F: Metal Physics* **15**, 1337 (1985).
- ²⁷I. Turek, V. Drchal, J. Kudrnovský, M. Sob, and P. Weinberger, *Electronic Structure of Disordered Alloys, Surfaces and Interfaces* (Kluwer Academic, Boston, 1997).
- ²⁸A. Liechtenstein, M. Katsnelson, V. Antropov, and V. Gubanov, *J. Magn. Magn. Mater.* **67**, 65 (1987).
- ²⁹M. Pajda, J. Kudrnovský, I. Turek, V. Drchal, and P. Bruno, *Phys. Rev. B* **64**, 174402 (2001).
- ³⁰P. Haas, F. Tran, and P. Blaha, *Phys. Rev. B* **79**, 085104 (2009).
- ³¹M. Hansen, *Constitution of Binary Alloys*, Metallurgy and Metallurgical Engineering Series (McGraw-Hill, New York, 1958).
- ³²S. K. Bose, J. Kudrnovský, V. Drchal, and I. Turek, *Phys. Rev. B* **82**, 174402 (2010).
- ³³J. Kudrnovský, F. Máca, I. Turek, and J. Redinger, *Phys. Rev. B* **80**, 064405 (2009).
- ³⁴L. M. Sandratskii, R. Singer, and E. Şaşıoğlu, *Phys. Rev. B* **76**, 184406 (2007).
- ³⁵M. A. Ruderman and C. Kittel, *Phys. Rev.* **96**, 99 (1954).
- ³⁶A. N. Yaresko, G.-Q. Liu, V. N. Antonov, and O. K. Andersen, *Phys. Rev. B* **79**, 144421 (2009).
- ³⁷ J_2' manifests itself in the AFM state. It gives rise to the difference in the values of the effective parameters between parallel and antiparallel pairs of Fe spins.
- ³⁸D. Stanek, O. P. Sushkov, and G. S. Uhrig, *Phys. Rev. B* **84**, 064505 (2011).
- ³⁹Y. Endoh and Y. Ishikawa, *J. Phys. Soc. Jpn.* **30**, 1614 (1971).
- ⁴⁰T. Jo, *J. Phys. F: Metal Physics* **13**, L211 (1983).
- ⁴¹M. W. Long, *J. Phys: Condens. Matter* **1**, 2857 (1989).

⁴²We also verified that the inclusion of SOC does not modify the present phase diagram.

⁴³J. Kouvel and J. Kasper, *J. Phys. Chem. Solids* **24**, 529 (1963).

⁴⁴S. Kawarazaki, K. Fujita, K. Yasuda, Y. Sasaki, T. Mizusaki, and A. Hirai, *Phys. Rev. Lett.* **61**, 471 (1988).

⁴⁵S. J. Kennedy and T. J. Hicks, *J. Phys. F: Metal Physics* **17**, 1599 (1987).

⁴⁶M. L. Winterrose, L. Mauger, I. Halevy, A. F. Yue, M. S. Lucas, J. A. Muñoz, H. Tan, Y. Xiao, P. Chow, W. Sturhahn, T. S. Toellner, E. E. Alp, and B. Fultz, *Phys. Rev. B* **83**, 134304 (2011).